

A Study on evaluation of chemokines and endoproteases in the human prostate cancer stem cells

Surampudi Sreedhar, Siva Kumar Kandula, Satyanarayana Swamy Cheekatla

Department of Biotechnology, GITAM Institute of Science (GIS) (Deemed to be University), Visakhapatnam, Andhra Pradesh, India

SUMMARY

Prostate cancer, the greatest cause of mortality among men, is a prevalent disease. CSC's role and paradigm in prostate cancer development and initiation has received a lot of attention in cancer biology since it provides insights into cancer pathophysiology and therapy responses. CSCs interact with their surroundings, altering cell fate by triggering key signaling regulators, culminating in a metastatic cascade. Chemokines and their receptors are involved in survival, proliferation, and invasion in primary and metastatic sites. According to recent data, these proteins work along with MMPs to improve tumour cell survival, proliferation, and metastasis in a multistep process. MMPs interact with host components to promote cancer growth. These could have a chemo-preventive effect on angiogenesis-related pathways such as stem cell markers and stem cell behaviour injunction. As a result, establishing a relationship between specific cell surface markers associated CSCs and MMPs aids in the development of prospective therapeutics and clinical trial-ready medications. Scant data is available to support the use of MMPs to prevent prostate cancer by counteracting CSC inactivation. The current study focused on the separation and characterization of PCa CSCs, in addition to the production of chemokines and MMPs. In isolated tertiary spheroidal Pca CSCs, there was prominent expression of CD133+ and CD44+ cell surface markers, as well as overexpression of OCT4 and ABCB1/MDR-1. CD133+44+ sub population were expressing significantly high SDF-1 α , CXCR-4 and endoproteases on comparison with primary cultures of normal prostate and CD133+ subpopulation. PCa CSC double positive subpopulation has a better survival rate and may be involved metastatic angiogenic progression.

Key words: CSC, metastasis, chemokines, MMPs, angiogenic tumors

INTRODUCTION

Despite advances in early detection and treatment of patients, modern oncotherapies offer few therapeutic options for those with locally advanced disease [1]. Because a large percentage of prostate cancer cells are testosterone-dependent, most people with advanced cancer will benefit from testosterone elimination therapy. Hormone-independent tumours with extensive metastases and a proclivity for hormone resistance are expected. The markers linked to stem cells in the basal, luminal, and neuroendocrine areas of the prostate tissue have been extensively studied. Many of the traits stated above will contribute to cancer growth, self-renewal capacity, and metastatic migration and extension, all of which will result in recurrence and cancer progression [2].

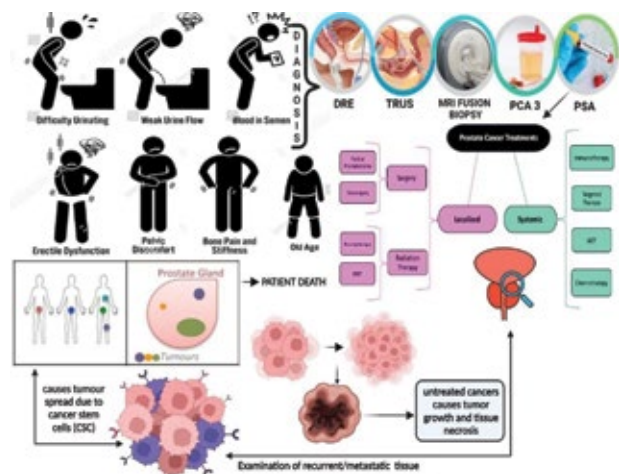


Fig.1. Prostate Cancer, signs, symptoms and its micro-environment

Normal prostate tissue stem cells have non-neoplastic properties. All healthy prostate stem cells do not need to be transformed into cancer stem cells [Figure 1]. Non-responsiveness will result in conversion to primary PCa CSCs. Cell-cell interactions, cellular pro-apoptotic signals, DNA repair, splicing mechanisms, hypermutations caused by chromosomal defects, and other processes are regulated by CSCs. Prostate CSCs have their own set of markers that may or may not be the same as those discovered in prostate stem cells. As a result, the creation and conversion of prostate CSC has become a contentious issue in the context of cancer relapse and treatment failure as shown in the [3]. Based on the centralised notion of changing normal stem cells into cancer, mouse model research has indicated that basal epithelial cells are more powerful in converting PCa. During orchidectomy, basal cells will be under control due

Address for correspondence:

Satyanarayana Swamy Cheekatla, Department of Biotechnology, Assistant Professor Department, GITAM Institute of Science (GIS) (Deemed to be University), Visakhapatnam, Andhra Pradesh, India

Word count: 8957 **Table:** 01 **Figures:** 08 **References:** 74

Received:- 20 April, 2022, Manuscript No. OAR-22-61365

Editor assigned:- 24 April, 2022, PreQC No. OAR-22-61365(PQ)

Reviewed:- 02 May, 2022, QC No. OAR-22-61365(Q)

Revised:- 04 May, 2022, Manuscript No. OAR-22-61365(R)

Published:- 05 May, 2022, Invoice No. J-OAR-OAR-22-61365

to normal maturation, while luminal cells will be completely eliminated due to apoptosis. As a result, prostatectomy has become a method for determining cancer stem cell mechanistic aversion. Testosterone replacement therapy encourages luminal progenitor cells to flourish and phenotypically evolve into castration-resistant prostate cancer [4-12].

Hematological cancers were used to demonstrate CSCs, while embryonic stem cell features were used to indicate their potential. Property-based specialized stem cells are found in every organ, and their CSCs are found in a variety of cancers. These cells are known as progenitor cells, and they may play a role in tumour growth and cancer relapse [13-18]. The nature of the tumour may differ from cancers in the same person and tumours of the same kind in multiple people.

CSCs are totipotent, self-renewing cells with characteristics similar to those of ordinary cells. Through symmetric and asymmetric division, these tumour cell subgroups demonstrate their dispersion and maintenance. The heterogeneous tumour is mostly made up of cancer stem cell descendants. Understanding the underlying interaction between neutral drift and dynamic modifications will aid our research into the various aspects of these malignancies. These studies will also help us understand the anti-metastatic tendency that occurs as a result of a planned clonal evolution sequence [19-28].

The ability of specific proteolytic systems known as matrix metalloproteinases to hydrolyze critical components of extracellular matrix barriers is the most important feature of the tumour microenvironment's niche. This aids tumour dispersion by allowing it to infiltrate neighbouring tissues via intravasation, extravasation, and metastasis. The goal of this study was to determine the key markers associated with CSC survivability in connection to the production of chemokines and various endoproteases.

AIM AND OBJECTIVES

This research aimed to find out the types of subpopulations in cancerous tissues and quantification of MMPs associated with chemokines when cultured.

- To isolate drug-resistant cancer stemcells from prostate cancer tissues
- To study the expression levels of Matrix metalloproteinases

MATERIALS AND METHODS

Patient sample collection

Tissue was obtained from 13 patients with symptomatic confined prostatic carcinoma, ranging from 44 to 79 years old. Patients in this study had prostate adenocarcinomas and had extensive retropubic catheterization with no signs of metabolic recurrence in the last year. Exclusion criteria included clinical manifestations at the initial diagnosis, a previous conviction of any malignancy, preemptive intervention, and the emergence of a recurrent malignant tumor. We chose a sample size of 6 patients from a total of 13 individuals, who met these criteria, and PSA serum levels were measured before and after prostate

surgery. One month following surgery, PSA serum levels were tested, and all patients had undetectable levels. Eight males (aged 24 to 42) were included in the study, all of whom had histologically normal (NP) prostates at dissection (8 hours-10 hours after death) and no history of reproductive, hormonal, or similar problems. Our institution's Ethics Committee accepted the study, which followed all requirements. Slices of two tissue cores of 2 mm thickness were obtained from the significant tumor mass of each carcinoma by cutting perpendicular to the urethra at the positive surgical margin from the center of the prostate gland. Following surgical removal, the slices were zipped in liquid nitrogen and remained at 80°C for an average of 15 minutes.

Tissue processing and cell suspension

Prostate cancer core biopsy with TRUS guidance cut and frozen tissue was mechanically triturated in a culture plate with 1 ml of 1x PBS at room temperature using a sterile scalpel and forceps. A sterile polystyrene conical tube was used to transfer 1 mL of suspension. The trituration procedure was carried out three to four times until all tissue slices were entirely dissociated. The dissociated contents were reconstituted and centrifuged at 3,200 rpm for 1 minute using a 5 ml serological pipette. The resulting suspension is filtered through a 35 m cell strainer to remove fibroblasts and used to isolate specific cell subpopulations and generate single-cell suspensions.

Magnetic activated cell sorting assay

The CD133-, CD133+44- adhering, and CD133+44+ were obtained using the MACS kit (Miltenyi Biotec, Germany). The entire population of cells was catalytically separated into a single cell solution and measured to determine the total number of cells. The cells (1×10^7) were treated for 30 minutes at 4°C with 100 µl microbeads conjugated to mouse monoclonal anti-human CD133 antibody. The dispersed cells were placed in a MACS column, which was then subjected to the magnetic field of a MACS separator. The CD133+ cells that had been tagged were kept on the column, and the untagged cells were decanted. Once the magnetic field was withdrawn from the column, the magnetically trapped CD133+44- cells were harvested as positive cells. The same procedure was repeated to generate CD133- and CD133+44+ cells using mouse monoclonal anti-human CD44 antibodies. Collected subpopulations were characterized by Flow cytometry.

Flow cytometric analysis

Antibodies against surface antigens such as FITC-CD133 (MiltenyiBiotec, Germany) and PE-CD44 (MiltenyiBiotec, Germany) were used to stain cells as directed by the manufacturer (MiltenyiBiotec, Germany). Primary cells were grown for 48 hours in 1% FBS before being trypsinized using 2.5% trypsin-EDTA (Gibco, USA), rinsed thoroughly in PBS, and incubated with 10 µl of antibodies in the dark for 30 minutes. The cells were permeabilized for 1 minute in PBS containing 0.1 percent Triton X-100 before being incubated with intracellular antibodies. The cell populations were then identified using

FACS (BD Bioscience, USA). The data gathered was assessed by Cell Quest Pro.

Cell culture

A T75 flask (ultra-low adherence) was used to cultivate MACS-enriched PCa tissue subpopulation cells and normal prostate tissue cells (Corning, France). The cells were suspended in 10 mL of CSC culture medium that contained DMEM/F12, glutamax (Life technologies), 4 g/mL of heparin (Sigma), 2% of B-27 supplement (Life technologies), 20 ng/mL of EGF, and FGF-b (Peprotech, Neuilly-sur-Seine, France), and 1% streptomycin. Fresh 20 ng/ml EGF and 10 ng/ml bFGF were added to the culture medium every other day (Peprotech).

Spheroid formation assay

CD133⁻, CD133⁺, and CD133⁺44⁺ subpopulations were grown in complete DMEM (Invitrogen, Frederick, MD). Trypsin was used to harvest 80 percent confluent cultures, which were then gently pipetted to create a single cell suspension for the spheroid formation experiment. The cells recovered by sedimentation at 2,000 rpm for 5 minutes were inactivated with trypsin inactivation in serum-containing media. Thousands of cells were resuspended in spheroid media containing 20 ng/ml EGF (Sigma, St. Louis), 2% of B-27 serum-free supplement (Invitrogen, Frederick, MD), 4 g/ml insulin (Sigma), and 0.4% BSA (Sigma). The cells were then seeded into six-well cluster dishes, which are ultra-low attachment cluster dishes (Corning, Tewksbury, MA). Spheres were checked regularly under a microscope, and detached cells were used to prepare a single-cell suspension for 4, 8, and 12 days after the sphere size reached $\geq 50 \mu\text{m}$. These were considered parental, secondary, and tertiary passages, and the time for sphere formation varied significantly based on the subpopulation. The number of passes from which the cells formed spheroids was indicated by the passage number, P1, P2, etc.

Colony formation assay

A single-cell suspension was generated from non-adherent tertiary passage culture and seeded on Petri plates after carefully counting cells in each sample using a hemocytometer with sufficient dilution (2000 cells/plate). Each subpopulation was seeded in triplicate on 15-mm dishes. The Petri dishes were placed in a humidified plastic cloning box for one week at 37°C with 5% CO₂. Cultures were washed in 5 mL of 0.9% saline after carefully removing the media from the culture plates by aspiration. For 15 to 30 minutes, colonies were immersed in 5 mL of 10% neutral buffer with formalin solution. After fixation, the cells were stained with crystal violet (5 mL of 0.01 percent-w/v) for 30 minutes-60 minutes, and the excess was rinsed with deionized water. Let the plates be allowed to dry. The colonies were counted using a stereomicroscope. Image J, an imaging analysis software tool, was used to estimate digital photographs of the colonies taken with a camera or scanning instrument. (1.53j version)

Cell viability and drug resistance

Tertiary cell suspensions from distinct CSC subpopulations were plated in 96-well plates (100 μl ; 4,000–5,000 cells per well) and cultured for 24 hours at 37°C with 5% CO₂ at saturated humidity. The media was then replaced, and the cultures were split into two groups: control and treatment, each with four parallel wells. The cultures in the treatment group were treated with 1 μM Doxorubicin for 12 and 24 h. Doxorubicin-treated cultured cells were stained with 5 μl of FITC-Annexin V in the dark for 30 minutes (at 10 μM concentration). The cells were incubated in the dark for another 10 minutes after the addition of PI (5 μl with a concentration of 10 μg per ml). The cells were filtered via a 35 μm mesh screen and analysed by flow cytometry.

Whole-cell lysate

The cells were rinsed with ice-cold PBS after tertiary cell suspensions from various CSC subpopulations were stored on ice. PBS should be removed and replaced with ice-cold lysis buffer (1 mL per 10⁷ cells in a 100 mm dish of 150 cm² flask; 0.5 mL per 5 \times 10⁶ cells in a 60 mm dish of 75 cm² flask). Using a cold plastic cell scraper, remove adhering cells from the plate and transfer the cell suspension to a pre-cooled microcentrifuge tube. The cell suspension was centrifuged at 12,000 rpm after 30 minutes of continuous agitation at 4°C. The tubes were kept on ice after being removed from the centrifuge. The supernatant was aspirated and stored at -80 degrees Celsius for further western blotting examination, while the cell pellet was discarded.

Concentration of cell culture supernatant

Tertiary cell suspensions prepared with distinct CSC subpopulations were cultured in serum-free DMEM for seven days. The cells were incubated in 20 ml of serum-free DMEM supplemented with 2 g/ml plasminogen at 37°C. The cell-free conditioned media was collected every 24 hours and replaced with fresh media. The TCA-NLS-THF precipitation method was used to concentrate the proteins in the conditioned media. The Bradford assay was used to measure the yield during protein recovery for every growth condition, and the sample data was compared to the reference standards of the BSA.

SODIUM DODECYL SULFATE POLYACRYLAMIDE GEL ELECTROPHORESIS (SDS-PAGE)

The components used for the SDS-PAGE technique are listed in Appendix 1. The gels were cast in this technique, with the production of the 8% resolving gel and 5% of stacking gel. TEMED was added for gel polymerization. Solidified prepared gels were immediately used or stored in moist paper (4°C) to carry out gel electrophoresis. Samples used in this technique are cell lysates and supernatants of concentrated cultures. Relevant samples were prepared by combining them in two times the amount of Laemmli buffer. Proteins were denatured by heating the mixer at 95°C for 5 minutes at 1,400 rpm on a shaker. The gel was run at 120 V with 200 mA maintained at

50 W for 70 minutes using a running buffer, and 15 µl-30 µl of the relevant samples were placed into the remaining gel pockets. The electrophoretic run was tracked using bromophenol blue tracking dye-containing Laemmli buffer.

Western blotting

The semi-dry blot method is used to transfer proteins from various SDS gels to nitrocellulose membranes. The proteins on the denaturing gel were transferred onto the membrane by blotting at 120 V (50 W) for 1 hour at 100 mA. Protein transfer onto the nitrocellulose membrane was tracked by staining with Ponceau Red, with a protein detection sensitivity of around 0.5–1 µg. Stained membranes were scanned, and the results were documented. The nitrocellulose membrane was initially treated with 2 percent skimmed milk dissolved in TBS-Tween to prevent non-specific antibody binding during the subsequent incubation procedures. The primary antibody was mixed with 2 percent skimmed milk (1:1000) in TBS-Tween for specific labeling of extracted protein. To remove unbound antibody molecules, the membranes were washed numerous times with TBS-Tween. The membrane was then treated with the species-specific secondary antibody, which was diluted (1:5000) in 2 percent skimmed milk dissolved in TBS-Tween. The membranes were washed, air-dried, and incubated for 1 minute at RT with ECL solution and then incubated in a dark-room. Later, membranes were exposed to photographic ECL Hyperfilms and the signals were measured using ImageJ. Blots were removed and reprobed with beta-actin (control) for equivalency. With appropriate calculations, the signals of the samples were normalised to be accurate with housekeeping proteins that had been loaded as an internal control for quantification.

Gelatin zymography

The presence of MMPs was studied by gelatin zymography. Cell supernatants free of cell debris were used in non-reducing SDS-PAGE zymography in gelatin-acrylamide gels. A 12% Bis-tris gel with 10% (w/v) of gelatin as a resolving gel and 3.9% of Bis-tris stacking gel was prepared for all gelatin zymography experiments. To this solution, freshly prepared 100 µl and 10 µL 10% APS (w/v final) and TEMED were added and pipetted the gel solution immediately into the gel casts. The gel was covered with an isopropyl alcohol layer to prevent evaporation, which was removed once the gel had set. The concentrated protein samples were prepared in the appropriate non-reducing buffer. Gel pockets were loaded with 15–30 µl of samples, and the gel was run at 120 V, 200 mA, and 50 W of running buffer. The gels are then washed overnight at 37°C with 2.5 percent, 50mM Triton X-100, and development buffer

for gelatin lysis. The lytic gels were destained and labelled with Coomassie brilliant blue (0.5%). The gelatinolytic activity, visualised as a white band against a blue backdrop, was imaged in ChemiDoc and quantified through ImageJ software. The enzyme activities of MMPs were calculated considering the ratio of the optical density of the experimental sample and the activity of 2 ng of rMMPs isolated on the same gel.

RESULTS

Isolation and Characterization of CSCs from human prostate cancer tissues

The potential cancer stem cell of prostate tissues following radical prostatectomy was determined. Six prostate cancer tissue suspensions were briefly analysed based on the inclusion and exclusion criteria mentioned in the materials and methods. Tissues were homogenised into cell suspensions. These cell suspensions were sorted for cell surface markers CD133 and CD44 by the magnet-associated cell sorting method (MACS) as described in materials and methods. Three phenotypic subpopulations were separated (CD133-, CD133+44- and CD133+44+ cells).

Individual live-cell subsets were counted, and [table 1] shows the median fraction of subsets to total cells in the tissue. As shown in the table and [figure 2], the median percentages of CD133, CD133+44- and CD133+44+ cells were found to be 89 (range, 85 to 96), 9 (range, 5.5 to 13.5), and 0.32 (range, 0.14 to 0.45), respectively, as shown in the table and [figure 3]. As shown in [figure 2] A, flow cytometry was used to verify the purity of the sorted CD133+44+ subpopulation and it was found to be more than 95%, as shown in [figure 2].

Self-renewal and sphere-forming ability in CSCs subsets

The proliferative capacity of the individual subpopulations was determined by culturing and serially passing them in DMEM stem cell-conditioned culture media as mentioned in the materials and methods. The CD133-, CD133+44- and CD133+44+ with a density of 1000 cells per well were plated in 24-well plates. All three subpopulations were developed as spheres, which are non-adherent clusters. When the spheres grew to a diameter of 50µm, they were passaged every four days, and the single-cell from the spheres was able to produce new spheres. This ability to create spheres was tested in parental and serially passaged sphere cultures. As shown in [Figure 3], CD133+ and CD133+44+ CSCs show a significant increase in the number

Tab.1. Expression of CSC markers in primary prostate tumors

| PATIENT | CD133 ⁺ | CD133 ⁺ 44 ⁻ | CD133 ⁺ 44 ⁺ |
|---------|--------------------|------------------------------------|------------------------------------|
| P1 | 92% | 7.5% | 0.39% |
| P2 | 86% | 9.5% | 0.35% |
| P3 | 90% | 8.5% | 0.29% |
| P4 | 88% | 11.2% | 0.23% |
| P5 | 85% | 13.5% | 0.14% |
| P6 | 96% | 5.5% | 0.45% |

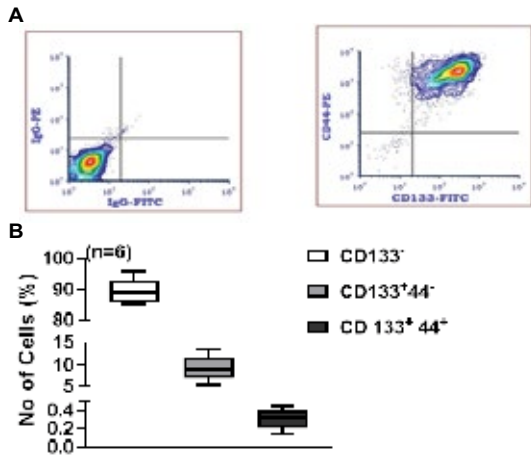


Fig.2. Percentage of CD133⁻, CD133⁺44⁻, CD133⁺44⁺ cells in primary prostate tumors (n=6) as determined by flow cytometry. Single-cell suspensions were prepared by magnetic sorting, followed by flow cytometric analysis. **A):** Representative flow cytometric plot. **B):** The relative variations in the frequency of each of the three sub-populations are depicted in box plots. The minimum and maximum values are represented by the whiskers, the median value is represented by the center lines, and the 25th and 75th percentiles are represented by the boxes

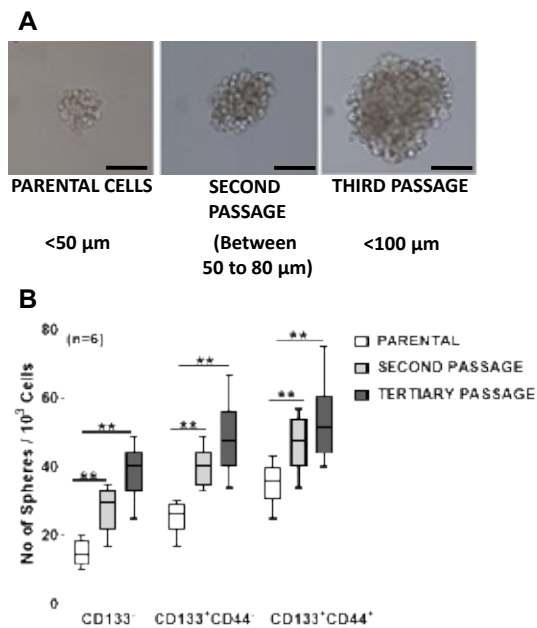


Fig. 3. The sphere-forming assay with human prostate cells. **A):** Representative bright-field images of human prostate spheres are shown. Scale bars=100 μm. **B):** Sphere formation (n=6) by CD133⁻, CD133⁺44⁻ and CD133⁺44⁺ cells culture on days 4, 8, and 12 of culture. The fraction of cells that form spheres is shown in box plots. The minimum and maximum values are represented by the whiskers, the median value is represented by the center lines, and the 25th and 75th percentiles are represented by the boxes. In contrast to parental cells, statistical significance was determined using a t-test test (* p<0.05, ** p<0.01, *** p<0.001)

of spheres and size (50 μm to 100 μm) compared to parental cultures. However, CD133⁻ cells did not show any apparent increase in the number of spheres upon passaging compared to their parental cultures.

Using a clonogenicity assay, we compared the proliferative potential of tertiary passaged spheres from three sub-populations. Two thousand cells were adherently plated and cultured for seven days. The cultures were stained with crystal violet and counted. CD133⁺44⁻ and CD133⁺44⁺ tertiary

sphere-forming cells proliferated much faster than CD133⁻ cells, resulting in significantly larger and more tumour colonies. When the number of colonies per 2,000 implanted cells is counted, there is no significant difference between CD133⁺44⁻ and CD133⁺44⁺ tertiary sphere-forming cells (48.5, 4.55, and 4.84 (P=0.05)) [Figure 4]. The sphere-forming cells were able to proliferate in large numbers and may play an important role in tumor formation.

Chemotherapy is often ineffective against prostate cancer. Prostate cancer stem cells are more likely to be resistant to therapy, which leads to recurrence. To determine their chemoresistance, the

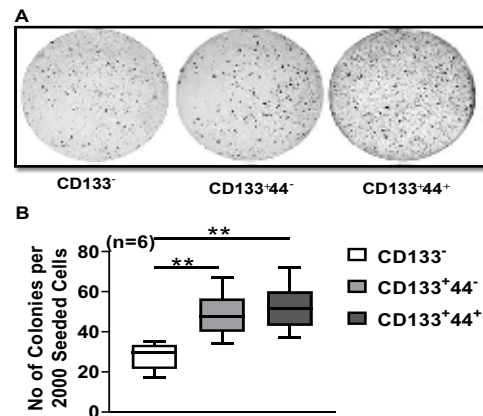


Fig.4. Sphere-forming cells proliferated extensively *in vitro*. **A):** Clonogenicity of tertiary sphere-forming cells (n=6). **B):** Cells were seeded in 6-well plates with a density of 2,000 cells per well and cultivated for one week. Proliferation efficiency was assessed through crystal violet staining and photographed. The percentage of proliferating cells is shown in box plots. The minimum and maximum values are represented by the whiskers, the median value is represented by the center lines, and the 25th and 75th percentiles are represented by the boxes. In contrast to CD133⁻ cells, statistical significance was determined using a t-test (* p<0.05, ** p<0.01, *** p<0.001)

sensitivity of CD133⁻, CD133⁺44⁻, and CD133⁺44⁺ tertiary sphere-forming cells to doxorubicin was studied. Doxorubicin-treated cultures at 24 h showed increased cell survivability when compared to parental. Relative survival rates differ significantly between the CD133⁺44⁻ and CD133⁺44⁺ subpopulations after 12 and 24 hours of culture when compared to the CD133⁻ subpopulation, as shown in [Figure 5] (P 0.05).

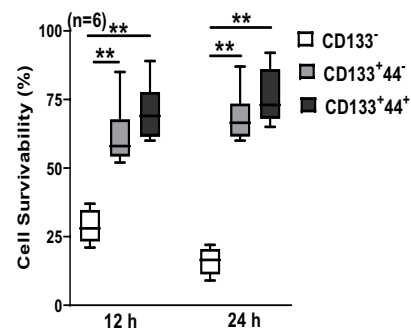


Fig.5. Doxorubicin treatment affects three subpopulations of cancer stem cells. Survivability of tertiary passaged CD133⁻, CD133⁺44⁻ and CD133⁺44⁺ spheroidal cells for 12 and 24 hours after Doxorubicin treatment (n=6). Box plots show the percentage of annexin-V positive cells. The minimum and maximum values are represented by the whiskers, the median value is represented by the center lines, and the 25th and 75th percentiles are represented by the boxes. Unlike CD133⁻ cells, a t-test was used to determine statistical significance (* p<0.05, ** p<0.01, *** p<0.001)

Sphere-forming cells overexpress stemness-related proteins

Cells of prostate cancerous tissue express related genes to stem cells like OCT-4 and ABCB1/MDR-1. Therefore, as described in the materials and methods chapter, we performed western blotting to look at the stem-ness-related protein expression levels. Compared to the CD133- subpopulation and normal prostate cells, both CD133+ and CD133+44+ tertiary spheroidal cells showed significant overexpression of OCT4 and ABCB1/MDR-1 stemness genes (p-value < 0.05) [Figure 6].

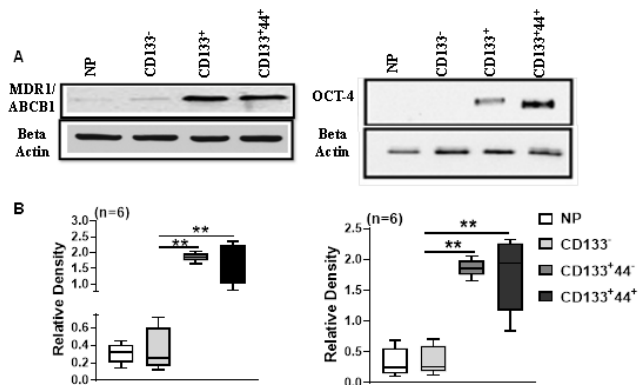


Fig.6. Expression of drug-resistant markers in the three subpopulations of cancer stem cells. **A):** A representative western blot showing the expression of MDR1/ABCB1 and OCT-4. The cellular extracts from the three subpopulations were prepared as stated in the materials and methods chapter. The extracts (40 µg of protein in each line) were separated on a 10% acrylamide gel. Expression levels of markers such as MDR1/ABCB1 and OCT-4 were determined by western blot (n=6). β-actin was used as a loading control. **B):** The relative expression of MDR1/ABCB1 and OCT-4 is shown in box plots. The minimum and maximum values are represented by the whiskers, the median value is represented by the center lines, and the 25th and 75th percentiles are represented by the boxes. In contrast to normal prostate cells, the statistical significance of the results was determined using a t-test (* p<0.05, ** p<0.01, *** p<0.001)

Determination of various MMPs and Chemokines in CD133+44+ CSC cultures

CSC breakdown, tumor neovascularization, and subsequent metastasis are mediated by MMPs. Depending on the target substrates, the MMP family is grouped into collagenases (1, 8, and 13), stromelysins (3 and 10), matrilysins (7), and gelatinases (2 and 9). We cultured CD133+ and CD133+44+ tertiary oncosphere cultures for seven days to see if they produced different MMPs and chemokines. The culture supernatants were concentrated using TCA-NLS-THF precipitation method filters as stated in the materials and methods section. The concentrated protein from the culture supernatants was then used to detect MMPs, and simultaneously, cell lysates were prepared to detect chemokines using western blotting and densitometry. CD133+44+ tertiary oncosphere cultures secreted elevated MMPs and chemokine proteins compared to CD133+ or normal prostate (NP) cultures [Figure 7 and 8], demonstrating the functional significance of CD133+44+ CSC subpopulation cells. The median representation after normalisation shows SDF-1 alpha (1.820, 1.63 to 1.96), CXCR-4 (1.86, 1.65 to

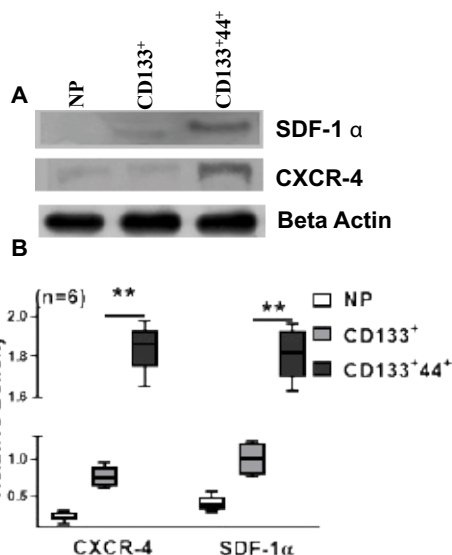


Fig.7. Expression of chemokines and their receptor in the Normal prostate and single, double-positive subpopulations of cancer stem cells. **A):** A representative western blot showing the expression of SDF-1 α and CXCR-4. The lysates of whole-cell extracts from the Normal prostate and two subpopulations were prepared as stated in the materials and methods chapter. The extracts (40 µg of protein in each line) were separated on a 10% acrylamide gel. Expression levels of SDF-1 α and CXCR-4 were determined by western blot (n=6). β-actin was used as a loading control. **B):** The relative expression of CXCR-4 and SDF-1 is shown in box plots. The minimum and maximum values are represented by the whiskers, the median value is represented by the center lines, and the 25th and 75th percentiles are represented by the boxes. In contrast to normal prostate cells, the statistical significance of the results was determined using a t-test (* p<0.05, ** p<0.01, *** p<0.001)

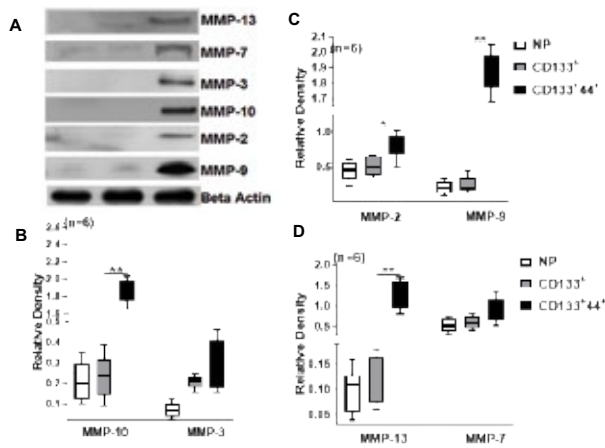


Fig.8. Expression of Matrix metalloproteinases (MMPs) - Gelatinases (MMP-9 & 2), Stromelysins (MMP-10 & 3), Collagenases (MMP-13) and Matrilysin (MMP-7) in the Normal Prostate and single, double-positive subpopulations of cancer stem cells. **A):** A representative western blot showing the expression of MMPs. The concentrated cell culture supernatants from the normal prostate and two subpopulations were prepared as stated in the materials and methods chapter. The extracts (40 µg of protein in each line) were separated on a 10% acrylamide gel. Expression levels of MMPs such as 13, 7, 3, 10, 2, and 9 were determined by western blot (n=6). β-actin was used as a loading control. **B, C & D):** The relative expression of MMPs is shown in box plots. The minimum and maximum values are represented by the whiskers, the median value is represented by the center lines, and the 25th and 75th percentiles are represented by the boxes. In contrast to normal prostate cells, the statistical significance of the results was determined using a t-test (* p<0.05, ** p<0.01, *** p<0.001)

1.98) in CD133+44+ whole cell lysates cultures. As shown in Figure 4.6B, the CD133+44+ subpopulation was expressed significantly higher than the CD133+ subpopulations of SDF-1 alpha (0.29 to 0.56 and 0.76 to 1.24) and chemokine receptor CXCR-4 (0.13 to 0.31 and 0.6 to 0.96) ($p < 0.05$).

In addition, MMP-2 (0.5 to 1.04) and MMP-9 (1.68 to 2.05) in CD133+44+ were significantly higher in comparison with CD133+ and primary cultures of normal prostates shown in figure 4.7B. A similar significant expression trend was observed in stromelysins (MMP 10 – 1.65 to 2.03; MMP 3 – 0.10 to 0.26), collagenases (MMP 13 – 0.8 to 1.7), and matrilysin (MMP 7 – 0.53 to 1.56) as shown in figures 4.7 C and D.

The polyclonal MMP antibodies used in western blotting recognise both pro and active forms of MMPs [Figure 8]. Proteinase activities in concentrated samples were detected by gelatin-zymography to confirm actual MMP activity [Figure 9]. Clear bands were visualised in CD133+44+ cell subpopulations than in normal prostate and CD133+, indicating increased MMP activity in the supernatants of CD133+44+ CSC subpopulation cells derived from prostate cancer. Zymography ($n=6$). Coomassie blue was used to stain the gels, and the active proteins were detected as clear lysis zones against a dark background. Expression levels of chemokines in lysates and all MMPs in supernatants were significantly higher in the CD133+44+ subpopulation. This subpopulation was cultured for further studies to study the angiogenic potential towards tumor progression.

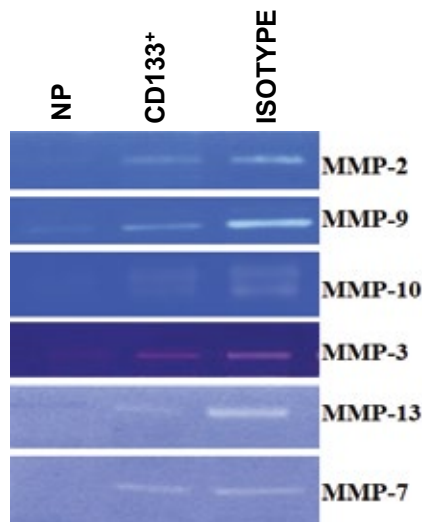


Fig.9. Expression of MMPs in the Normal Prostate and single, double-positive subpopulations of cancer stem cells. A representative Gelatin Endoprotease zymogram was shown. The concentrated cultured supernatants from the Normal prostate and single (CD133+), double-positive subpopulations (CD133+44+) were prepared as stated in the materials and methods chapter. The extracts (40 µg of protein in each line) were separated on a 10% gelatinized acrylamide gel. Gelatinolytic activity of MMPs was determined by Gelatin Zymography ($n=6$). Coomassie blue was used to stain the gels, and the active proteins were detected as clear lysis zones against a dark background.

DISCUSSION

Tumor growth and angiogenesis are aided by the presence of solid tumour matrix, necessary proteases, and pro-angiogenic

factors. Cancer metastasis occurs when cancer cells from the original tumour spread to other organs in the body, causing morbidity and mortality. Proteases such as MMPs regulate cell shape and activity during metastatic tumour progression by breaking down extracellular matrix and cleaving basement membrane components. Early metastatic maintenance is aided by MMPs, which generate intravasation and maintain neovasculature during tumour growth. MMPs also help to maintain the health of blood vessels, which helps to prevent the formation of distant secondary tumours during the progression of prostate cancer. Because of its local invasiveness, lymph node malignancy, and resistance to traditional therapy, PCa has a bad prognosis. Despite recent advances in surgical technology and adjuvant drugs, unfavourable diagnosis as a replica has been reported following PCa therapy [29-31]. CSCs' importance in cancer recurrence and metastatic spread has been supported by their identification and targeted eradication as a viable PCa therapeutic method. The current study looked at how PCSCs and MMPs interact during tumor mediated metastatic angiogenesis. PCSCs are the primary targets in cancer therapy because they are the driving force behind carcinogenesis and metastasis. A number of CSC markers have recently been found in a variety of solid and hematopoietic malignancies [32-34]. CSCs are a subset of cancer cells that exhibit multiple surface markers such as CD133 and CD44 and make up the majority of cancer cells in both solid and non-solid tumours [35-38]. The markers CD133 and CD44 [39-40], which are associated with poor prognosis in invasive in vitro studies because of their high expressions, are found in very well-known isolated and identified CSCs [41-48]. Using CD133 or CD44 as a diagnostic marker, CSCs were recently found in primary laryngeal cancer cells, LSCC, and PCa malignant cells [49-56]. According to Hermanns and Collins' research, pancreatic and prostate cancer cells that are CD133+/CXCR4+ and CD44+/α2β1hi/CD133+ are tumorigenic [57-60]. As a result, CSCs aid tumour growth and dissemination.

CSC Isolation and its characterization from prostate tissues

Select biomarkers, which are usually found on the cell surface, can be used to identify CSCs [61]. The most prevalent isolation procedures (MACS) are FACS and MACS [62]. FACS technology has been widely employed in cancer, immunology, neuroscience, and stem cell research since Dick JE initially used it to screen CSCs for leukaemia [63]. MACS is a simple and inexpensive alternative to FACS for retaining cell viability [64]. According to previous research [64], CSCs in head and neck SCC show considerable expression of surface markers such as CD133 and CD44. In the current work, MACS was utilised to identify CD133 and CD44 double-positive subpopulation cells from PCa, which were then examined by flow cytometry in the current work. MACS was used to examine the properties of CD133 and CD44 associated cells isolated from Pca patient tissues (CD133+44+ cells vs CD133+44-, CD133-44+, CD133-44- cell subpopulations and parental cells). Due to particular drug-resistant cell surface phenotypic markers like MDR-1 (ABCB1) and OCT-4, the CSCs of various solid tumours show great resistance to chemotherapeutic drugs.

Drug-resistant indicators trigger tumour relapse by expelling cytotoxic medicines that are required for cell survival and tumour invasiveness [47]. CSCs efficiently express multidrug resistance proteins such as ABC transporters (ABCB1, ABCC1, and ABCG2), which protect leukaemia and other solid tumour cells from treatment by acquiring drug resistance, according to Gottesman et al. [34-36]. Cancer CSC cells have high levels of OCT-4, a critical stem cell factor that controls morphogenesis and differentiation capacity. The majority of studies discovered a link between OCT-4 expression and chemoresistance, which is associated with a poor clinical outcome [56]. Assessing CSC medication resistance is critical to avoid disruptions in cancer treatment. Doxorubicin is a widely used palliative chemotherapy drug for hormone-refractory prostate tumours. Drug resistance was stronger in CD133+44+ cells compared to CD133-44+, CD133+44-, and parental cells. MDR-1 and OCT-4 expression are higher in CD133+44+ cells. As a result, CD133+44+ cells could be a suitable target for anticancer and PCa therapies. To better understand the distinctions between CD133+ and CD44+ PCa CSCs, CD133+ and CD44+ cells were concentrated in parental and drug-treated tertiary passaged cells. CSCs have two distinct properties: self-renewal and chemo-resistance [34]. Furthermore, chemotherapeutic resistance was found to be higher in CD133+44+ cells than in CD133+ or CD44+ cells by themselves. In serum-free circumstances, CD133+44+ cells form spheres reliably. It was surprising that CD133+44+ cells demonstrated a higher rate of self-renewal and colony formation than CD133+ or CD44+ cells, which was surprising [46]. Surface markers and the ability to form spheres are two characteristics of CSCs. [21]. CD133+44+ (PCSCs) subpopulations were found to have more stemness, malignancy, and tumorigenicity than other subpopulations (CD133+44-, CD133-44+), as well as parental cells.

According to new evidence and cohort studies, chemokines and their receptors are implicated in a multistep process during PCSC survival, proliferation, and invasion, making the tumour more aggressive and resistant to therapy. Controlling or inhibiting chemokines or their receptors could be useful markers for reducing PCSC-mediated tumour development. CXCR-4 is a chemokine receptor found in most human malignancies but not in normal epithelial cells. According to Xueqing Sun [32], CXCR-4 has been identified in numerous tumours during the mediation of tumour spread and works as a biomarker for tumour behaviour [61]. In many malignancies, including CXCL12/SDF-1 in PCa, a CXCR-4 related ligand promotes PCSC tumour growth and metastasis. Increased expression of SDF-1alpha and CXCR-4 in prostate cancer patients indicates bone metastases [34-36]. Dubrovskaja and Singh et al. found that high levels of CXCR-4 and SDF-1 alpha in double-positive PCa cell cultures encourage distant organ metastasis indirectly by modulating proliferation, differentiation likelihood, and tumorigenicity [37]. Because CSCs can initiate metastasis and cause relapse during primary treatment, antibody inhibition of CXCR-4 and SDF-1 lowers the size of the tumour and the number of CSCs [60-63]. In comparison to other cell subpopulations, our western blotting data revealed increased chemokine expression in PCSCs of tertiary passaged oncospheres.

Because of the role of MMPs in cancer, we focused on cytokines and growth factors involved in increasing prostate cancer cell migration in conjunction with PCa CSC-mediated MMPs. With the involvement of MMPs and chemokines, studies on the carcinogenic and angiogenic capacity of PCa CSCs were conducted. In a mouse model, CXCR-4 regulation and knockdown reduce bone metastases and impact the production of VEGF and MMPs in PC-3 cells [23]. Chemokines regulate MMP participation in various stages of metastasis, such as invasion and extravasation. ECM degradation and subsequent rearrangement caused by MMPs MMP expression was found to be 30 times higher in malignant prostate tissues than in nonmalignant prostate tissues in several studies. Tumor adversity was found to have a substantial positive connection with MMPs in a variety of solid tumours, particularly as a predictor of prostate cancer. Or and colleagues [65]. discovered that in MMP-8 neutralised mice, the absence of MMP promotes tumorigenesis by enhancing cutaneous carcinogenesis sensitivity [66]. MMP expression in PCSC-grown oncospheres is thus still unknown. The goal of this study was to detect MMP in the tumour niche, which could be involved in matrix and tissue border cleavage, which leads to angiogenic development. According to numerous studies, proteases have been implicated in a variety of odd malignancies. MMP-2 activity levels are thought to be prognostic [67], and their involvement in pathogenesis is unknown. Regardless of disease stage, PSA, or GS, MMP-2 overexpression in malignant prostate glands has been demonstrated to be a greater predictor of prostate cancer than disease-free survival [68]. Protease levels, particularly MMP-2 and 9, are associated with tumour stemness and aggressiveness in the PCSC subpopulation of a prostate tumour [69]. Decreased levels of MMP-2 and its regulators have also been associated with prostate cancer [70], whereas Sabrina Thalita et al. found that MMP-3 is positively related to cancer invasiveness and metastasis. MMP-7, a protease capable of cleaving basement membrane, is thought to be linked to cancer [71-73]. According to Sugure Maruta's research, MMP-10 was predominantly found in the cytoplasm of cancer cells, and its expression in cancer cells (13.8%) was substantially higher than in non-tumoral cells (2.4%) [73]. MMP-10 disrupts the growth and death of cancer cells, contributing to the progression of non-metastatic prostate cancer. MMP-7, on the other hand, suppresses angiogenesis in HUVECs by blocking the VEGF pathway [74]. MMP-2, 8, and 9 activation in ECs is activated by chemokines and cytokines with known pro-angiogenic characteristics, therefore regulating angiogenesis [74].

CONCLUSION

In this investigation, PCSC cultured supernatants had significantly higher quantities of gelatinolytic proteases than non-tumoral cells, as seen by clear visual bands. We can speculate that increased MMP expression is responsible for profile elucidation in PCa tissue and might be a characteristic of prostate cancer that can be utilised for tumor diagnosis.

- REFERENCES
- Dubrovskaya A, Elliott J, Salamone RJ, Teleguev GD, Stakhovskiy AE, et al. CXCR4 expression in prostate cancer progenitor cells. *PLoS One*. 2012; 7.
 - Yamamoto A, Kasamatsu A, Ishige S, Koike K, Saito K, et al. Exocyst complex component Sec8: A presumed component in the progression of human oral squamous-cell carcinoma by secretion of matrix metalloproteinases. *J. Cancer Res. Clin. Oncol.* 2013; 139:533–542.
 - Timmermans AJ, Gooijer CJD, Vrieze OH, Hilgers FJM, Brekel MWMVD. T3-T4 laryngeal cancer in The Netherlands Cancer Institute; 10-year results of the consistent application of an organ-preserving/-sacrificing protocol. *Head & Neck*. 2015; 37:1495-1503.
 - Goldstein AS, Huang J, Guo C, Garraway IP, Witte ON. Identification of a cell of origin for human prostate cancer. *Science*. 2010; 329:568-571.
 - Atena M, Reza AM, Mehran G. A Review on the Biology of Cancer Stem Cells. *Stem Cell Res*. 2014; 4:83–89.
 - Furusato B, Mohamed A, Uhlén M, Rhim JS. CXCR4 and cancer. *Pathol. Int*. 2010; 60:497-505.
 - Bonnet D, Dick JE. Human acute myeloid leukemia is organized as a hierarchy that originates from a primitive hematopoietic cell. *Nat Med*. 1997; 3:730–737.
 - Odoux C, Fohrer H, Hoppo T, Guzik L, Stolz DB. A stochastic model for cancer stem cell origin in metastatic colon cancer. *Cancer Res*. 2008; 68:6932–6941.
 - Zhong C, Wu JD, Fang MM, Pu LY. Clinicopathological significance and prognostic value of the expression of the cancer stem cell marker CD133 in hepatocellular carcinoma: A meta-analysis. *Tumour Biology. Int J Dev Biol*. 2015; 36:7623–7630.
 - Lynch CC, Hikosaka A, Acuff HB, Martin MD, Kawai N. MMP-7 promotes prostate cancer-induced osteolysis via the solubilization of RANKL. *Cancer Cell*. 2005; 7:485-496.
 - Gourin CG, Dy SM, Herbert RJ, Blackford AL, Quon H. Treatment, survival, and costs of laryngeal cancer care in the elderly. *The Laryngoscope*. 2014; 124:1827-1835.
 - Xin HC, Ying Z, Liang DG, Fen YJ, Yang LZ, et al. Screening for MiRNAs related to laryngeal squamous carcinoma stem cell radiation. *Asian Pac. J. Cancer Prev*. 2013; 14:4533-4537.
 - Mitri DD, Toso A, Chen JJ, Sarti M, Pinton S, et al. Tumour-infiltrating Gr-1+ myeloid cells antagonize senescence in cancer. *Nature*. 2014; 515:134–137.
 - Horst D, Scheel SK, Liebmann S, Neumann J, Maatz S, et al. The cancer stem cell marker CD133 has high prognostic impact but unknown functional relevance for the metastasis of human colon cancer. *J. Pathol*. 2009; 219:427-434.
 - Lawson DA, Xin L, Lukacs RU, Witte ON. Isolation and functional characterization of murine prostate stem cells. *PNAS*. 2007; 104:181-186.
 - Rudolph E, Dyckhoff G, Becher H, Dietz A, Ramroth H. Effects of tumour stage, comorbidity and therapy on survival of laryngeal cancer patients: A systematic review and a meta-analysis. *European Archives of Oto-Rhino-Laryngology: Eur Arch Otorhinolaryngol*. Affiliated with the German Society for Oto-Rhino-Laryngology -Head and Neck Surgery. 2011; 268:165–179.
 - Chu EA, Kim YJ. Laryngeal cancer: Diagnosis and preoperative work-up. *Otolaryngol. Clin. North Am*. 2008; 41:673-695. [Google Scholar] [Cross Ref]
 - Yun EJ, Lo UG, Hsieh JT. The evolving landscape of prostate cancer stem cell: Therapeutic implications and future challenges. *Asian J Urol*. 2016; 3:203-210.
 - Cara GD, Marabeti MR, Musso R, Riili I, Cancemi P, et al. New Insights into the Occurrence of Matrix Metalloproteases -2 and -9 in a Cohort of Breast Cancer Patients and Proteomic Correlations. *Cells*. 2018; 7.
 - Morgia G, Falsaperla M, Malaponte G, Madonia M, Indelicato M, et al. Matrix metalloproteinases as diagnostic (MMP-13) and prognostic (MMP-2, MMP-9) markers of prostate cancer. *Urol Res*. 2005; 33:44-50.
 - Marchenko GN, Ratnikov BI, Rozanov DV, Godzik A, Deryugina EI, et al. Characterization of matrix metalloproteinase-26, a novel metalloproteinase widely expressed in cancer cells of epithelial origin. *Biochem J*. 2001; 35:705-718.
 - Clevers H. Stem cells, asymmetric division and cancer. *Nat. Genet*. 2005; 37:1027-1028.
 - Long H, Xiang T, Qi W, Huang J, Chen J, et al. CD133+ ovarian cancer stem-like cells promote non-stem cancer cell metastasis via CCL5 induced epithelial-mesenchymal transition. *Oncotarget*. 2015; 6:5846-5859.
 - Mochizuki H, Matsubara A, Teishima J, Mutaguchi K, Yasumoto H, et al. Interaction of ligand-receptor system between stromal-cell-derived factor-1 and CXC chemokine receptor 4 in human prostate cancer: A possible predictor of metastasis. *Biochem Biophys Res Commun*. 2004; 320:656-663.
 - Valli H, Sukhwani M, Dovey SL, Peters KA, Donohue J, et al. Fluorescence- and magnetic-activated cell sorting strategies to isolate and enrich human spermatogonial stem cells. *Fertil Steril*. 2014; 102: 566-580.
 - Chen J, Zhou J, Lu J, Xiong H, Shi X, et al. Significance of CD44 expression in head and neck cancer: A systemic review and meta-analysis. *BMC Cancer*. 2014; 14.
 - Han J, Fujisawa T, Husain SR, Puri RK. Identification and characterization of cancer stem cells in human head and neck squamous cell carcinoma. *BMC Cancer*. 2014; 14.
 - Visvader JE, Lindeman GJ. Cancer stem cells in solid tumours: Accumulating evidence and unresolved questions. *Nat Rev Cancer*. 2008; 8:755-768.
 - Freije JMP, Balbín M, Pendás AM, Sánchez LM, Puente XS, et al. Matrix metalloproteinases and tumor progression. *Adv Exp Med Biol*. 2003; 532:91-107.
 - Medema JP. Cancer stem cells: The challenges ahead. *Nat Cell Biol*. 2013; 15:338-344.
 - Hashimoto K, Kihira Y, Matuo Y, Usui T. Expression of matrix metalloproteinase-7 and tissue inhibitor of metalloproteinase-1 in human prostate. *J Urol*. 1998; 160:1872-1876.
 - Rycak K, Tang DG. Molecular determinants of prostate cancer metastasis. *Oncotarget*. 2017; 8: 88211-88231.
 - Harris KS, Kerr BA. Prostate Cancer Stem Cell Markers Drive Progression, Therapeutic Resistance, and Bone Metastasis. *Stem Cells Int*. 2017; 2017:1-9.
 - Wang L, Guo H, Lin C, Yang L, Wang X. Enrichment and characterization of cancer stem-like cells from a cervical cancer cell line. *Mol Med Rep*. 2014; 9:2117-2123.
 - Xin L, Lawson DA, Witte ON. The Sca-1 cell surface marker enriches for a prostate-regenerating cell subpopulation that can initiate prostate tumorigenesis. *PNAS*. 2005; 102: 6942-6947.
 - Kokko LL, Hurme S, Maula SM, Alanen K, Grénman R, et al. Significance of site-specific prognosis of cancer stem cell marker CD44 in head and neck squamous-cell carcinoma. *Oral Oncol*. 2011; 47:510-516.
 - Cojoc M, Peitzsch C, Trautmann F, Polishchuk L, Teleguev GD, et al. Emerging targets in cancer management: Role of the CXCL12/CXCR4 axis. *OncoTargets Ther*. 2013; 6:1347—1361.
 - Germann M, Wetterwald A, Ramirez NG, der Pluijm GV, Culig Z, et al. Stem-like cells with luminal progenitor phenotype survive castration in human prostate cancer. *Stem Cells*. 2012; 30:1076-1086.
 - Geens M, de Velde HV, Block GD, Goossens E, Steirteghem AV, et al. The efficiency of magnetic-activated cell sorting and fluorescence-activated cell sorting in the decontamination of testicular cell suspensions in cancer patients. *Hum Reprod*. 2007; 22: 733-742.
 - Miyake M, Goodison S, Lawton A, Giacoia EG, Rosser CJ. Angiogenin promotes tumoral growth and angiogenesis by regulating matrix metalloproteinase-2 expression via the ERK1/2 pathway. *Oncogene*. 2015; 34: 890-901.
 - Prince ME, Sivanandan R, Kaczorowski A, Wolf GT, Kaplan MJ, et al. Identification of a subpopulation of cells with cancer stem cell properties in head and neck squamous cell carcinoma. *PNAS*. 2007; 104:973-978.
 - Gottesman MM, Fojo T, Bates SE. Multidrug resistance in cancer: Role of ATP-dependent transporters. *Nat Rev Cancer*. 2002; 2:48-58.
 - Cardillo MR, Silverio FD, Gentile V. Quantitative immunohistochemical and in situ hybridization analysis of metalloproteinases in prostate cancer. *Anticancer Res*. 2006; 26: 973-982.
 - Karatas OF, Suer I, Yuceturk B, Yilmaz M, Hajiyev Y, et al. The role of miR-145 in stem cell characteristics of human laryngeal squamous cell carcinoma Hep-2 cells. *Tumour Biol*. 2016; 37: 4183-4192.
 - Mook ORF, Frederiks WM, Noorden CJFV. The role of gelatinases in colorectal cancer progression and metastasis. *Biochim Biophys Acta*. 2004; 1705:69-89.
 - Camarero P, Lombardo Y, Francipane MG, Bonventre S, Todaro M, et al. Isolation and culture of colon cancer stem cells. *Methods Cell Biol*. 2008; 86:311-324.

47. Kunz P, Sähr H, Lehner B, Fischer C, Fellenberg ESJ. Elevated ratio of MMP2/MMP9 activity is associated with poor response to chemotherapy in osteosarcoma. *BMC Cancer*. 2016; 16.
48. Xia P. Surface markers of cancer stem cells in solid tumors. *Curr Stem Cell Res Ther*. 2014; 9:102-111.
49. Sarvaiya PJ, Guo D, Ulasov I, Gabikian P, Lesniak MS. Chemokines in tumor progression and metastasis. *Oncotarget*. 2013; 4:2171-2185.
50. Shah PK, Shah KK, Karakousis GC, Reinke CE, Kelz RR, et al. Regional recurrence after lymphadenectomy for clinically evident lymph node metastases from papillary thyroid cancer: A cohort study. *Ann Surg Oncol*. 2012; 19:1453–1459.
51. Wang Q, Diao X, Sun J, Chen Z. Stromal cell-derived factor-1 and vascular endothelial growth factor as biomarkers for lymph node metastasis and poor cancer-specific survival in prostate cancer patients after radical prostatectomy. *Urol Oncol*. 2013; 31:312-317.
52. Fukushima R, Kasamatsu A, Nakashima D, Higo M, Fushimi K, et al. Overexpression of Translocation Associated Membrane Protein 2 Leading to Cancer-Associated Matrix Metalloproteinase Activation as a Putative Metastatic Factor for Human Oral Cancer. *J Cancer*. 2018; 9:3326-3333.
53. Pardal R, Clarke MF, Morrison SJ. Applying the principles of stem-cell biology to cancer. *Nat Rev Cancer*. 2003; 3:895–902.
54. Xu R, Cai MY, Luo RZ. The Expression Status and Prognostic Value of Cancer Stem Cell Biomarker CD133 in Cutaneous Squamous Cell Carcinoma. *JAMA Dermatol*. 2016; 152:305-311.
55. Reis ST, Antunes AA, Junior JP, Canavez JMDS, Oglio MFD, et al. Underexpression of MMP-2 and its regulators, TIMP2, MT1-MMP and IL-8, is associated with prostate cancer. *Int Braz j Urol*. 2012; 38:167–174.
56. Maruta S, Miyata Y, Sagara Y, Kanda S, Iwata T, et al. Expression of matrix metalloproteinase-10 in non-metastatic prostate cancer: Correlation with an imbalance in cell proliferation and apoptosis. *Oncol Lett*. 2010; 1:417-421.
57. Singh S, Chellappan S. Lung cancer stem cells: Molecular features and therapeutic targets. *Mol Asp Med*. 2014; 39: 50-60.
58. Singh S, Singh UP, Grizzle WE, Lillard JW. CXCL12-CXCR4 interactions modulate prostate cancer cell migration, metalloproteinase expression and invasion. *Lab Invest J Tech Methods Pathol*. 2004; 84:1666–1676.
59. Lang SH, Frame FM, Collins AT. Prostate cancer stem cells. *J Pathol*. 2009; 217:299-306.
60. Sahlberg SH, Spiegelberg D, Glimelius B, Stenerlöw B, Nestor M. Evaluation of cancer stem cell markers CD133, CD44, CD24: Association with AKT isoforms and radiation resistance in colon cancer cells. *PLoS One*. 2014; 9.
61. Morrison SJ, Kimble J. Asymmetric and symmetric stem-cell divisions in development and cancer. *Nature*. 2006; 441:1068-1074.
62. Baek SK, Jung KY, Kang SM, Kwon SY, Woo JS, et al. Clinical risk factors associated with cervical lymph node recurrence in papillary thyroid carcinoma. *Thyroid Off J Am Thyroid Assoc*. 2010; 20: 147-152.
63. Lapidot T, Sirard C, Vormoor J, Murdoch B, Hoang T, et al. A cell initiating human acute myeloid leukaemia after transplantation into SCID mice. *Nature*. 1994; 367:645–648.
64. Reya T, Morrison SJ, Clarke MF, Weissman IL. Stem cells, cancer, and cancer stem cells. *Nature*. 2001; 414:105–111.
65. Ito TK, Ishii G, Saito S, Yano K, Hoshino A, et al. Degradation of soluble VEGF receptor-1 by MMP-7 allows VEGF access to endothelial cells. *Blood*. 2009; 113:2363-2369.
66. Pozzi V, Sartini D, Rocchetti R, Santarelli A, Rubini C, et al. Identification and characterization of cancer stem cells from head and neck squamous cell carcinoma cell lines. *Cell Physiol Biochem Int J Exp Cell Physiol Biochem Pharmacol*. 2015; 36:784-798.
67. Plaks V, Kong N, Werb Z. The cancer stem cell niche: How essential is the niche in regulating stemness of tumor cells?. *Cell Stem Cell*. 2015; 16:225-238.
68. Sun X, Cheng G, Hao M, Zheng J, Zhou X, et al. CXCL12 / CXCR4 / CXCR7 chemokine axis and cancer progression. *Cancer Metastasis Rev*. 2010; 29:709–722.
69. Chen XH, Bao YY, Zhou SH, Wang QY, Wei Y, et al. Glucose transporter-1 expression in CD133+ laryngeal carcinoma Hep-2 cells. *Mol Med Rep*. 2013; 8:1695-1700.
70. Bi Y, Meng Y, Wu H, Cui Q, Luo Y, et al. Expression of the potential cancer stem cell markers CD133 and CD44 in medullary thyroid carcinoma: A ten-year follow-up and prognostic analysis. *J Surg Oncol*. 2016; 113:144-151.
71. Mayea YG, Mir C, Masson F, Paciucci R, LLeonart ME. Insights into new mechanisms and models of cancer stem cell multidrug resistance. *Semin Cancer Biol*. 2020; 60:166-180.
72. Jung Y, Wang J, Schneider A, Sun YX, Paige AJK, et al. Regulation of SDF-1 (CXCL12) production by osteoblasts; a possible mechanism for stem cell homing. *Bone*. 2006; 38:497-508.
73. Xing Y, Liu M, Du Y, Qu F, Li Y, et al. Tumor cell-specific blockade of CXCR4/SDF-1 interactions in prostate cancer cells by hTERT promoter induced CXCR4 knockdown: A possible metastasis preventing and minimizing approach. *Cancer Biol Ther*. 2008; 7:1839-1848.
74. Vincent Z, Urakami K, Maruyama K, Yamaguchi K, Kusuhara M. CD133-positive cancer stem cells from Colo205 human colon adenocarcinoma cell line show resistance to chemotherapy and display a specific metabolomic profile. *Genes Cancer*. 2014; 5:7–8.